Tetrahedron: *Asymmetry* 20 (2009) 89–97

Contents lists available at ScienceDirect

Tetrahedron: *Asymmetry*

journal homepage: www.elsevier.com/locate/tetasy

# Conformational study of (*R*)-(+)-limonene in the liquid phase using vibrational spectroscopy (IR, Raman, and VCD) and DFT calculations

Francisco Partal Ureña, Juan Ramón Avilés Moreno, Juan Jesús López González *

*Department of Physical and Analytical Chemistry, Experimental Sciences Faculty, University of Jaén, Campus Las Lagunillas, E-23071 Jaén, Spain*

ARTICLE INFO

*Article history:*
Received 26 September 2008
Accepted 23 January 2009
Available online 23 February 2009

ABSTRACT

A conformational study in the liquid phase of the terpene (*R*)-(+)-limonene has been carried out, revealing the presence of three conformers. For this task, experimental vibrational techniques, such as IR, Raman, and VCD spectroscopies, together with quantum chemical calculations, have been used. Our study reveals that a previous vibrational analysis is desirable to achieve a thorough analysis of the VCD spectrum as well as that these three experimental techniques are complementary to characterize flexible systems, which present several conformers.



## 1. Introduction

Chiral monoterpenes are usually used to test VCD devices, because of their availability in suitable enantiomer purity and their high-quality vibrational spectra in the mid-IR region.[1,2] Monoterpenes are also components of citrus fruits, olive oil, cherries, spearmint dill, caraway, apricots, grapes, and herbs, which means that they are consumed by humans in their daily diet. They show antitumor, antimicrobial, and antioxidant activities,[3–8] and their properties have given rise to work dealing with the study of the relationship of molecular structure/activity.[4,9] Furthermore, they are atmospheric pollutants[10,11] and have important uses as flavorings and perfumes,[9] as well as in the production of solvents and adhesives showing important biomedicinal applications. From this point of view, a deep knowledge of the molecular structure and possible conformers of this type of compounds would be desirable.

In the literature, papers dealing with the vibrational study of terpenoids are scarce, with only one dealing with cyclohexene-derived terpenoides, a study on the carvone molecule.[12] Recently, our group has carried out work dealing with the application of vibrational spectroscopy to the detection of conformers in the case of the terpenoid perillaldehyde.[13] In contrast, comparative work dealing with interpretations, from both experimental and theoretical points of view, of the VCD spectrum of terpenes, the title compound (*R*)-(+)-limonene (4-isopropenyl-1-methylcyclohexene, Fig. 1) being one of them, in the mid-IR[14–16] and near-IR[17–20] regions, can be found.

In the work of Polavarapu et al.,[14] the vibrational optical activity of some six-membered-ring monoterpenes was carried out, and they proposed that the vibrations of the ring methylenes are responsible for the major VCD features in the mid-IR range.

Later, Singh and Keiderling[15] carried out a theoretical interpretation of the VCD spectra of these types of molecules using the Fixed Partial Charge (FPC) method. For this, a conformational study by means of the Consistent Force Field (CFF) was made, with it being described for limonene an axial conformer and two equatorial conformers (referring to the isopropylene group position with respect to the ring) as the most stable ones. They showed that the VCD spectra of axial and equatorial conformers were nearly opposite in sign, and corroborated the interpretation that was previously made by Polavarapu et al.[14]

Lipp and Nafie[16] applied the Fourier self-deconvolution to interpretation of the VCD spectra of limonene as an example of this technique for retrieving information lost through band overlap, since limonene presents a severely congested spectrum.

Finally, work by Abbate et al.[18–20] dealt with interpretation of the VCD spectra in the overtones range in terms of local-modes behavior versus normal-modes behavior.

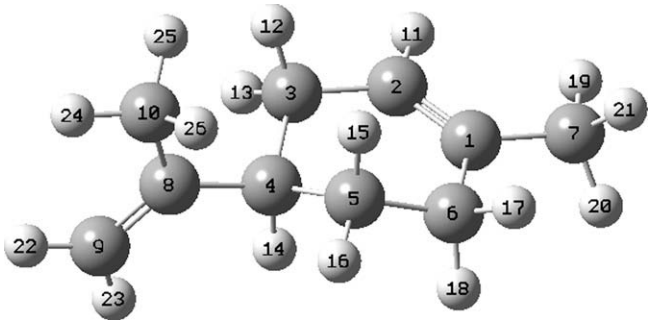


**Figure 1.** Molecular structure and atom numbering adopted in this study for the (*R*)-(+)-limonene, where the C4 is the chiral atom.

* Corresponding author. Fax: +34 953212940.
*E-mail address:* jjlopez@ujaen.es (J. J. López González).

0957-4166/$ - see front matter © 2009 Elsevier Ltd. All rights reserved.
doi:10.1016/j.tetasy.2009.01.024

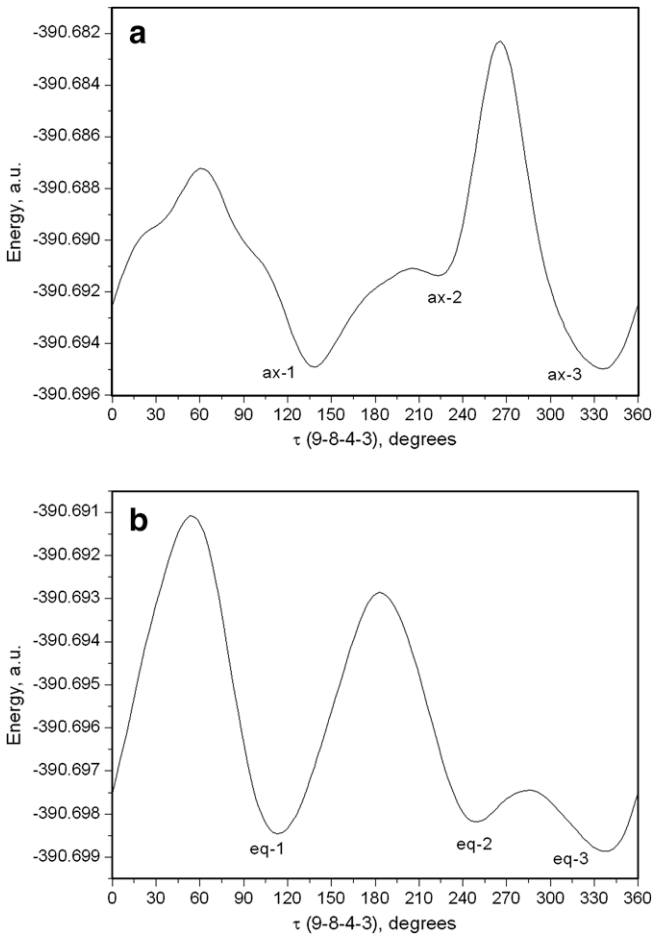


**Figure 2.** PES of the (*R*)-(+)-limonene molecule: (a) axial conformer, (b) equatorial conformer.

Herein, we report a conformational study of (*R*)-(+)-limonene. For this task, quantum chemical calculations at the DFT level of theory are carried out to characterize all the conformers that the title molecule presents in the gas phase. Afterwards, the most abundant conformers in the liquid phase were detected using vibrational (IR, Raman, and VCD) techniques.

## 2. Results and discussion

### 2.1. Molecular structure in the isolated molecule approach

From the fixed scan at the B3LYP/6-31G(d,p) level, three rotamers were found as energy minima of the PES for both equatorial and axial conformers (Fig. 2). The geometry optimization at the B3LYP/cc-pVDZ level of theory for the equatorial rotamers gave values for the torsion angle of the isopropenyl group with respect to the ring of 109.3° (eq-1), 247.3° (eq-2), and 338.0° (eq-3). For the axial rotamers, these values were 136.6° (ax-1), 221.8° (ax-2), and 340.1° (ax-3). The rotation of the methyl group around the C1–C7 simple bond gave rise to 3 equiv conformations. The variation of the rest of geometrical parameters from one rotamer to another rotamer is almost negligible (see Fig. 3).

This level of calculation also revealed that equatorial conformers are the most abundant with around 96% of the whole population. Relative energies and Boltzmann's populations are shown in Table 1. These results are in agreement with previous studies on a similar chemical system, the carvone (5-isopropenyl-2-methylcyclohex-2-en-1-one)[12,28,29] and with our previous work on perillaldehyde (4-isopropenylcyclohex-1-ene-1-carbaldehyde).[13]

### 2.2. Vibrational analysis

The molecular structure and vibrational spectra of the cyclohexene molecule have been studied from both theoretical and experimental points of view,[30–39] and there is a work dealing with the IR spectrum of the isopropenyl group in different molecular systems.[40] Nevertheless, work dealing with the molecular structure and vibrational spectra of cyclohexene-based terpenes, as a family of compounds, is not common in the literature, with the work developed by Hoffmann on cavone[12] and the work developed by our group on perillaldehyde[13] being the only ones reported around the vibrational spectra of this kind of systems.

(*R*)-(+)-limonene has $3N - 6 = 3 \times 26 - 6 = 72$ vibrational normal modes belonging to the unique irreducible representation (A) of its symmetry point group, $C_1$. Recorded IR and Raman

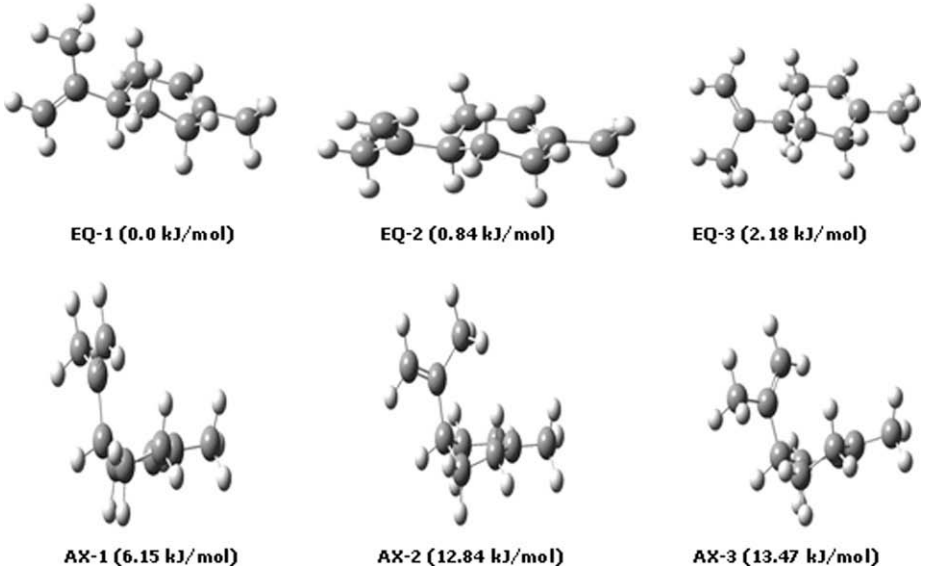


**Figure 3.** Structure of the six most stable conformers of the (*R*)-(+)-limonene at the B3LYP/cc-pVDZ level of theory. Relative energies taking into account the ZPE corrections are shown for each one.

**Table 1**
Calculated relative energies taking into account the ZPE correction ($\Delta E_0$) and corresponding Boltzmann's populations (considering $T = 298.16$ K) of the three equatorials and the three axial conformers of the (*R*)-(+)-limonene at the B3LYP/cc-pVDZ level of theory in the gas phase

| Conformer | $\Delta E_0$ (kJ mol$^{-1}$) | % Population |
|---|---|---|
| Eq-1 | 0.00 | 42.78 |
| Eq-2 | 0.69 | 32.38 |
| Eq-3 | 1.71 | 21.42 |
| Ax-1 | 13.41 | 0.19 |
| Ax-2 | 14.58 | 0.12 |
| Ax-3 | 6.49 | 3.11 |

spectra of (*R*)-(+)-limonene are displayed in Figure 4, and wavenumbers and relative intensities are listed in Table 2. In Table 3, the theoretical, scaled and experimental wavenumbers of the three equatorial conformers are shown. To obtain the scaled wavenumbers, the SQMFF methodology by Pulay et al.[24] was used. Thus, the cartesian hessian obtained from the DFT calculations was transformed into a new hessian in terms of Pulay's natural internal coordinates.[24] Afterwards, by using a MOLVIB program,[25,26] the theoretical wavenumbers were fitted to the experimental ones by means of a refinement process of the scale factors associated with the force constants in terms of natural internal coordinates. The refinement begins with a value of 1.000 for every scale factor. In the refinement procedure, experimental bands mainly coming from IR spectrum in liquid phase were taken into account. When IR bands were not present in the liquid phase, Raman bands were used. The description of every normal mode from the Potential Energy Distribution (PED) Matrix is also obtained in this process.

The predicted spectra after the scaling procedure, when taking into account the relative population of the three equatorial rotamers in the gas phase, are displayed in Figure 4. In Table 4 the sets of refined scaling factors for each of the rotamers of the equatorial conformer of (*R*)-(+)-limonene, as well as the set of their mean values, obtained in the refinement procedure for the B3LYP/cc-pVDZ level of theory are shown. The root mean square deviation (rms) obtained for the difference between the experimental and theoretical (after the refinement) wavenumber values of (*R*)-(+)-limonene using these scaling factors is 5.88 cm$^{-1}$, with the individual r.m.s.d. for each rotamer being 5.49 cm$^{-1}$ (EQ-1), 6.09 cm$^{-1}$ (EQ-2), and 6.04 cm$^{-1}$ (EQ-3).

(*R*)-(+)-Limonene displays complex and overlapped IR and Raman spectra. Herein, for the sake of clarity, the vibrational assignment is discussed, by dividing the complete mid-IR spectroscopic range into several zones.

### 2.2.1. C–H stretching region

This region shows a significant band overlapping, a feature also shown by the cyclohexene molecule,[30–39] where Fermi resonances between methylene C–H bond stretchings and combinations involving low-wavenumber modes are described for this region.[39] One of these Fermi resonances in the (*R*)-(+)-limonene spectrum is the experimental band observed at 2833 cm$^{-1}$ in the liquid IR and at 2836 cm$^{-1}$ in the Raman liquid (see Table 2).

The three bands appearing at higher wavenumbers in the IR spectrum are assigned to the C–H stretchings associated with the vinyl group and the C–C double bond in the ring (Table 2). Thus, from the results of the scaling procedure, the experimental band at 3084 cm$^{-1}$ in the IR spectrum and at 3085 cm$^{-1}$ in the Raman one is assigned to the normal mode 1 of EQ-2 and EQ-3, whose description from the PED is the asymmetric C–H stretching of the vinyl group (see Table 3). The experimental band at 3073 cm$^{-1}$ in the IR and Raman spectra can be assigned to the normal mode 1 of EQ-1, with the same description from the PED. The experimental band at 3011 cm$^{-1}$ in the IR spectrum and at 3013 cm$^{-1}$ in the Raman one can be assigned to normal mode 2 of EQ-1 and normal mode 3 of EQ-2 and EQ-3, which are described as the asymmetric C–H stretching corresponding to the C–C double bond in the ring. The normal mode 2 of EQ-2 and EQ-3 cannot be assigned to any experimental band and only its scaled value is known (Table 3). This assignment is in agreement with the one proposed for (*S*)-(−)-perillaldehyde.[13]

These three bands are the first examples of the presence of different rotamers in the neat liquid phase. They are also an example of an important feature of the experimental spectra of (*R*)-(+)-limonene,

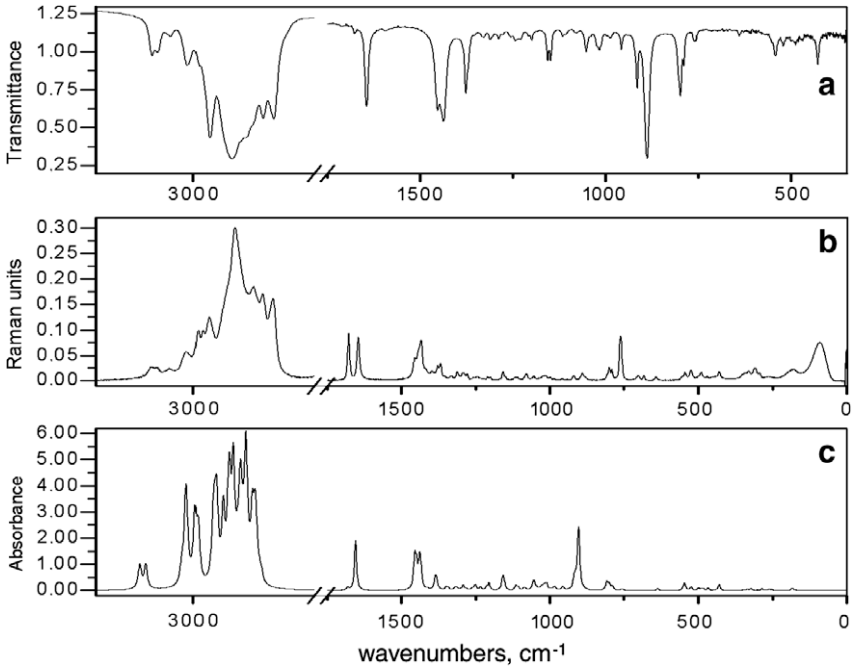


**Figure 4.** Experimental IR (a) and Raman (b) spectra (1 cm$^{-1}$ of resolution, 200 scans and neat liquid) compared with predicted scaled spectrum (c) for the (*R*)-(+)-limonene. (JASCO software package[27] was used to reproduce the predicted spectrum, pitch = 1 cm$^{-1}$, fwhm = 8 cm$^{-1}$).

**Table 2**
Experimental IR and Raman bands of (*R*)-(+)-limonene (in $cm^{-1}$) in the liquid phase[a]

| IR liquid | Intensity | Raman liquid | Intensity |
|---|---|---|---|
| 3084 | m | 3085 | w |
| 3073 | m | 3073 | w |
| 3046 | m | 3047 | w |
| 3011 | s | 3013 | w |
| | | 2989 | m |
| 2986 | s | | |
| | | 2980 | m |
| 2965 | s | 2966 | m |
| 2920 | vs | 2914 | vs |
| 2903 | br | | |
| 2895 | s | | |
| | | 2876 | s |
| 2856 | s | 2856 | m |
| 2833 | s | 2836 | m |
| 2766 | m | | |
| 2741 | sh | | |
| 2725 | m | 2728 | w |
| 2698 | sh | | |
| 2667 | m | | |
| 2643 | m, br | | |
| 2615 | m, br | | |
| 2590 | m, br | | |
| 2564 | m | | |
| 2523 | m, br | | |
| 2472 | m | | |
| 1780 | m | | |
| 1676 | s | 1678 | m |
| 1645 | s | 1646 | m |
| 1452 | s | 1455 | w |
| 1437 | s | 1434 | m |
| 1406 | w | | |
| 1397 | w | 1397 | w |
| 1392 | w | | |
| 1376 | s | 1378 | w |
| | | 1367 | w |
| 1356 | m | 1355 | w |
| 1338 | m | | |
| 1332 | m | | |
| 1327 | m | 1329 | w |
| 1310 | m | 1311 | w |
| 1288 | m | 1290 | w |
| 1277 | m | 1277 | w |
| 1254 | m | 1257 | w |
| 1243 | m | 1245 | w |
| 1227 | m | | |
| 1206 | m | 1208 | w |
| 1199 | m | 1198 | w |
| 1184 | w | | |
| 1155 | m | 1157 | w |
| 1147 | m | | |
| 1115 | m | 1114 | w |
| 1107 | m | | |
| 1078 | m | 1079 | w |
| 1052 | m | 1053 | w |
| 1040 | m | | |
| 1022 | sh | | |
| 1016 | m | 1016 | w, br |
| 996 | w | 997 | w |
| 986 | m | | |
| 957 | m | 959 | w |
| 940 | m | | |
| 914 | s | 918 | w |
| 887 | s | 889 | w |
| 797 | s | 799 | w |
| 789 | m | 789 | w |
| 758 | m | 761 | m |
| | | 702 | w |
| 679 | w | 682 | w |
| 668 | m | | |
| 640 | m | 642 | w |
| 570 | m | | |
| | | 554 | sh |
| 542 | m | 543 | w |
| 521 | m | 523 | w |
| 497 | m | | |
| 488 | m | 490 | w |
| 469 | m | 472 | w |
| 428 | m | 431 | w |
| | | 343 | w |
| | | 331 | w |
| | | 309 | w |
| | | 295 | w |
| | | 265 | w |
| | | 176 | w |

[a] Wavenumbers in $cm^{-1}$. Symbols: v = very, s = strong, m = medium, w = weak, br = broad, sh = shoulder.

the change in the description of some normal modes depending on the rotamers, also in agreement with (*S*)-(−)-perillaldehyde.[13]

Due to the significant overlapping of this zone, some normal modes that should appear cannot be assigned to any experimental band and several normal modes must be assigned to the same experimental band (see Table 3). These modes are described as motions of the methyl and methylene groups. In the next section, the assignment of these normal modes will be clarified with the aid of the VCD spectrum.

### 2.2.2. Spectroscopic region from 1700 $cm^{-1}$ to 400 $cm^{-1}$

The band with the highest wavenumber in this zone, observed at 1676 $cm^{-1}$ in the IR spectrum and at 1678 $cm^{-1}$ in the Raman spectrum is assigned in all the rotamers to the normal mode 17, whose description from the PED is the C=C bond stretching of the ring. The band observed at 1645 $cm^{-1}$ in the IR spectrum and at 1646 $cm^{-1}$ in the Raman spectrum is assigned to the normal mode 18, which is described as the C=C bond stretching of the vinyl group mixed with the symmetric deformation of the H–C–H angle of the same group to some extent (Tables 2 and 3).

The rest of the normal modes in this region present a complex description from the PED and are described as motions due to angle deformations of the methylene groups mixed with other vibrations due to the ring, C–C bond stretchings, and angle deformations of the substituent isopropenyl and methyl groups, in good agreement with the previous assignment on cyclohexene,[25,27,28,33] and in agreement with (*S*)-(−)-perilladehyde.[13] From the PED, it is found that in this region there are changes in the description of some normal modes from one rotamer to another rotamer. Likewise, and from our scaling calculation, different normal modes must be assigned to the same experimental band as, for example, normal mode 19 in EQ-1 and EQ-3 and normal modes 20 and 21 in all the rotamers, assigned to the band at 1452 $cm^{-1}$ in the IR spectrum, and normal mode 22 in EQ-3 and normal modes 23, 24, and 25 in all the rotamers, assigned to the band at 1437 $cm^{-1}$. In addition, some normal modes cannot be assigned to any experimental band, as for example normal mode 22 in EQ-1 and EQ-2.

Finally, from a detailed comparison between the experimental and theoretical spectra, the existence of different rotamers can be inferred. Thus, by taking into account the three most stable rotamers, a suitable reproduction of the spectroscopic profile can be achieved and some experimental bands assigned to an individual rotamer. As an example, normal mode 37, described as methylene scissoring motions mixed with the rocking of the C–H bond of the chiral carbon in all the rotamers, is assigned to the experimental band at 1206 $cm^{-1}$ for EQ-1 and EQ-3 and at 1199 $cm^{-1}$ for EQ-2 (see Tables 2 and 3).

### 2.2.3. Low-frequency vibrations region

The third region into study corresponds to the vibrations below 400 $cm^{-1}$. As in the previous region, normal modes present a

**Table 3**
Experimental, theoretical (B3LYP/ cc-pVDZ), and scaled wavenumbers (in $cm^{-1}$)

| MODE | EQ-1 | | | EQ-2 | | | EQ-3 | | |
|---|---|---|---|---|---|---|---|---|---|
| | Theoretical | Scaled | Experimental | Theoretical | Scaled | Experimental | Theoretical | Scaled | Experimental |
| 1 | 3220.3 | 3096,6 | 3073 | 3233.5 | 3109,5 | 3084 | 3231.7 | 3107,8 | 3084 |
| 2 | 3133.8 | 3013,6 | 3011 | 3143.5 | 3022,9 | | 3142.9 | 3022,3 | |
| 3 | 3130.6 | 3010,5 | 3011 | 3133.7 | 3013,6 | 3011 | 3136.2 | 3016,0 | 3011 |
| 4 | 3115.6 | 2996,0 | | 3114.9 | 2995,3 | | 3115.6 | 2996,0 | |
| 5 | 3108.8 | 2989,5 | 2989 | 3108.7 | 2989,3 | 2989 | 3108.9 | 2989,6 | 2989 |
| 6 | 3078.2 | 2960,0 | 2965 | 3075.3 | 2957,4 | 2965 | 3074.8 | 2956,9 | 2965 |
| 7 | 3069.6 | 2951,9 | | 3071.2 | 2953,3 | | 3067.7 | 2950,0 | |
| 8 | 3055.4 | 2938,1 | | 3055.5 | 2938,2 | | 3055.2 | 2937,9 | |
| 9 | 3041.6 | 2925,0 | | 3043.3 | 2926,6 | | 3045.1 | 2928,3 | |
| 10 | 3033.8 | 2917,5 | 2920 | 3033.9 | 2917,5 | 2920 | 3033.6 | 2917,4 | 2920 |
| 11 | 3024.8 | 2908,9 | 2914 | 3018.5 | 2902,8 | 2903 | 3018.5 | 2902,8 | 2903 |
| 12 | 3019.8 | 2904,0 | 2903 | 3017.3 | 2901,7 | 2903 | 3016.2 | 2900,5 | 2903 |
| 13 | 3012.7 | 2897,1 | 2895 | 3007.2 | 2891,9 | 2895 | 3006.7 | 2891,6 | 2895 |
| 14 | 3007.0 | 2891,8 | 2895 | 2992.7 | 2878,0 | 2876 | 3002.7 | 2887,5 | |
| 15 | 2993.4 | 2878,6 | 2876 | 2986.3 | 2871,8 | 2876 | 2984.3 | 2869,9 | 2876 |
| 16 | 2987.6 | 2873,0 | 2876 | 2973.5 | 2859,4 | 2856 | 2977.9 | 2863,7 | 2856 |
| 17 | 1743.8 | 1681,0 | 1676 | 1744.9 | 1682,1 | 1676 | 1744.1 | 1681,3 | 1676 |
| 18 | 1714.8 | 1654,2 | 1645 | 1715.8 | 1655,4 | 1645 | 1716.7 | 1656,3 | 1645 |
| 19 | 1471.8 | 1459,0 | 1452 | 1474.6 | 1461,7 | | 1470.4 | 1457,7 | 1452 |
| 20 | 1468.2 | 1455,7 | 1452 | 1466.7 | 1454,2 | 1452 | 1464.9 | 1452,3 | 1452 |
| 21 | 1461.2 | 1448,5 | 1452 | 1461.4 | 1448,7 | 1452 | 1461.8 | 1449,1 | 1452 |
| 22 | 1453.3 | 1441,1 | | 1452.8 | 1440,3 | | 1450.6 | 1438,4 | 1437 |
| 23 | 1450.5 | 1438,0 | 1437 | 1450.6 | 1438,3 | 1437 | 1450.4 | 1437,9 | 1437 |
| 24 | 1449.1 | 1436,7 | 1437 | 1449.6 | 1437,5 | 1437 | 1449.1 | 1436,9 | 1437 |
| 25 | 1445.7 | 1433,4 | 1437 | 1445.9 | 1433,5 | 1437 | 1443.9 | 1431,4 | 1437 |
| 26 | 1431.6 | 1416,6 | 1406 | 1428.5 | 1411,8 | 1406 | 1427.3 | 1411,1 | 1406 |
| 27 | 1398.9 | 1385,9 | 1376 | 1401.9 | 1388,3 | 1376 | 1401.3 | 1387,4 | 1376 |
| 28 | 1396.7 | 1383,4 | 1376 | 1398.9 | 1384,8 | 1376 | 1399.3 | 1384,9 | 1376 |
| 29 | 1388.8 | 1374,7 | 1376 | 1393.4 | 1380,9 | 1376 | 1392.1 | 1379,8 | 1376 |
| 30 | 1378.8 | 1365,3 | 1367 | 1388.3 | 1373,9 | 1367 | 1388.6 | 1374,0 | 1367 |
| 31 | 1360.5 | 1349,5 | 1356 | 1353.1 | 1341,8 | 1332 | 1358.2 | 1347,6 | 1356 |
| 32 | 1327.2 | 1316,5 | 1327 | 1333.1 | 1322,1 | 1327 | 1329.7 | 1319,2 | 1327 |
| 33 | 1317.0 | 1307,2 | 1310 | 1322.9 | 1312,3 | 1310 | 1323.9 | 1311,5 | 1310 |
| 34 | 1303.3 | 1291,6 | 1288 | 1307.9 | 1297,5 | | 1310.3 | 1300,8 | |
| 35 | 1297.1 | 1280,9 | 1277 | 1270.6 | 1258,8 | 1254 | 1274.2 | 1263,0 | |
| 36 | 1264.0 | 1253,1 | 1254 | 1261.7 | 1249,9 | 1243 | 1245.7 | 1233,5 | 1227 |
| 37 | 1226.0 | 1215,0 | | 1215.5 | 1204,7 | 1199 | 1222.8 | 1211,9 | 1206 |
| 38 | 1173.1 | 1156,9 | 1155 | 1176.0 | 1159,5 | 1155 | 1176.4 | 1160,2 | 1155 |
| 39 | 1162.4 | 1153,2 | 1155 | 1164.0 | 1154,9 | 1155 | 1161.0 | 1151,6 | 1147 |
| 40 | 1124.8 | 1106,5 | 1107 | 1133.4 | 1115,1 | 1115 | 1131.5 | 1113,8 | 1115 |
| 41 | 1093.7 | 1083,1 | 1078 | 1098.0 | 1087,4 | 1078 | 1090.0 | 1079,7 | 1078 |
| 42 | 1066.3 | 1053,2 | 1052 | 1070.2 | 1057,7 | 1052 | 1066.7 | 1051,2 | 1052 |
| 43 | 1057.4 | 1044,5 | 1040 | 1049.9 | 1037,5 | 1040 | 1057.1 | 1045,8 | 1052 |
| 44 | 1038.9 | 1029,3 | 1040 | 1039.2 | 1026,8 | 1022 | 1038.9 | 1029,1 | 1040 |
| 45 | 1026.7 | 1014,3 | 1016 | 1032.9 | 1021,8 | 1022 | 1032.3 | 1019,1 | 1016 |
| 46 | 1023.2 | 1009,5 | 1016 | 1009.7 | 998,3 | 996 | 1005.9 | 994,9 | 996 |
| 47 | 993.2 | 984,6 | 986 | 993.9 | 982,0 | 986 | 997.2 | 985,4 | 986 |
| 48 | 969.8 | 955,7 | 957 | 970.8 | 957,6 | 957 | 966.3 | 951,9 | 957 |
| 49 | 928.7 | 917,2 | 914 | 929.4 | 917,6 | 914 | 931.2 | 919,1 | 914 |
| 50 | 925.5 | 911,8 | 914 | 927.5 | 914,0 | 914 | 925.9 | 914,2 | 914 |
| 51 | 919.8 | 903,9 | | 917.8 | 901,8 | | 916.3 | 900,2 | |
| 52 | 892.8 | 877,1 | 880 | 902.2 | 885,1 | 887 | 904.3 | 886,9 | 887 |
| 53 | 815.7 | 806,0 | 797 | 817.3 | 809,1 | 797 | 817.5 | 807,4 | 797 |
| 54 | 798.4 | 787,8 | 789 | 812.2 | 798,9 | 789 | 806.3 | 795,1 | 789 |
| 55 | 767.3 | 752,7 | 758 | 773.1 | 758,4 | 758 | 769.6 | 755,1 | 758 |
| 56 | 730.5 | 699,7 | 702 | 712.1 | 683,7 | 679 | 711.6 | 682,9 | 679 |
| 57 | 645.9 | 635,4 | 640 | 646.4 | 635,9 | 640 | 643.9 | 633,7 | 640 |
| 58 | 554.1 | 545,5 | 542 | 551.3 | 542,9 | 542 | 557.5 | 549,1 | 542 |
| 59 | 528.7 | 521,9 | 521 | 530.1 | 523,5 | 521 | 505.9 | 499,3 | 497 |
| 60 | 494.3 | 488,6 | 488 | 488.7 | 483,1 | 488 | 496.4 | 490,7 | 488 |
| 61 | 473.1 | 467,9 | 469 | 447.2 | 442,2 | | 454.2 | 449,3 | |
| 62 | 434.4 | 429,9 | 428 | 433.5 | 429,1 | 428 | 435.1 | 430,5 | 428 |
| 63 | 339.1 | 335,3 | 331 | 351.1 | 347,4 | 343 | 340.0 | 336,4 | 331 |
| 64 | 326.3 | 323,0 | | 326.8 | 323,5 | | 320.7 | 317,7 | 309 |
| 65 | 288.3 | 285,3 | | 304.3 | 300,4 | 295 | 306.8 | 302,8 | 295 |
| 66 | 253.9 | 252,1 | | 263.2 | 261,3 | | 270.6 | 268,7 | 265 |
| 67 | 203.7 | 202,2 | | 201.2 | 199,5 | | 199.1 | 197,1 | |
| 68 | 184.3 | 183,4 | 176 | 183.9 | 183,3 | 176 | 186.8 | 185,8 | 176 |
| 69 | 181.1 | 180,4 | 176 | 178.0 | 175,9 | 176 | 184.2 | 183,3 | 176 |
| 70 | 169.9 | 167,8 | | 173.4 | 172,9 | 176 | 160.9 | 159,5 | |
| 71 | 72.5 | 72,2 | | 77.2 | 76,8 | | 81.1 | 80,6 | |
| 72 | 60.9 | 60,7 | | 44.7 | 44,5 | | 34.0 | 34,0 | |

**Table 4**
Developed sets of scaling factors for the three rotamers of (*R*)-(+)-limonene at the B3LYP/cc-pVDZ level, mean value and comparison with those obtained for (*S*)-(+)-perillaldehyde[13]

| Scaling factor | Limonene | | | | Perillaldehyde |
|---|---|---|---|---|---|
| | EQ-1 | EQ-2 | EQ-3 | Mean value | |
| C=C stretching | 0.913 | 0.912 | 0.914 | 0.913 | 0.902 |
| C–C stretching | 0.962 | 0.960 | 0.959 | 0.961 | 0.961 |
| C–H stretching | 0.926 | 0.925 | 0.925 | 0.925 | 0.923 |
| XYZ bending | 0.981 | 0.993 | 0.966 | 0.980 | 1.009 |
| Torsions of single-bonded systems | 0.995 | 1.003 | 0.980 | 0.993 | 0.981 |
| XY–H bending | 0.993 | 0.977 | 0.990 | 0.987 | 0.977 |
| Out-of-plane modes | 0.962 | 0.963 | 0.970 | 0.965 | 0.980 |
| H–X–H bending | 0.981 | 0.984 | 0.984 | 0.983 | 0.978 |
| Torsions of conjugated systems | 0.909 | 0.908 | 0.908 | 0.908 | 0.940 |
| C=O stretching | – | – | – | – | 0.890 |

complex description from the PED analysis, where waggings, rockings, and torsions of the substituent groups and of the ring and ring deformations appear mixed to some extent. As in the previous regions, some normal modes cannot be assigned to any experimental band; in Table 3, only their scaled values are shown. Likewise, different normal modes must be assigned to the same band. This is the case, for example, of the normal modes 68 and 69, in all the rotamers, and mode 70, in EQ-2, which are assigned to the band at 176 $cm^{-1}$ in the Raman spectrum.

In the reproduction of the spectroscopic features of this region, it is necessary to take into account the presence of the three equatorial rotamers. Although, as seen above, in some cases the same experimental band must be assigned to different normal modes of several rotamers, there are other experimental bands that can be assigned to only normal modes belonging to one rotamer. For example, the experimental band at 343 $cm^{-1}$ is assigned to normal mode 63 of EQ-2, and the band at 309 $cm^{-1}$ is assigned to normal mode 64 of EQ-3 (see Table 3).

### 2.3. VCD spectrum analysis

In the same way as in the vibrational analysis section, the study of the VCD spectrum will be divided into regions, in accordance with the detectors used in the recording of the spectrum described in the experimental section, that is, 3200–2800 $cm^{-1}$ (InSb) and 2000–900 $cm^{-1}$ (MCT-V).

#### 2.3.1. Spectroscopic region from 3200 $cm^{-1}$ to 2800 $cm^{-1}$

As in the case of the IR and Raman spectra studied in the previous section, the experimental VCD spectrum shows a great signal overlapping. This feature was already pointed out in the previous work by Polavarapu et al.[14] The recorded experimental spectrum in $CCl_4$ solution by these authors was studied in the region between 3000 $cm^{-1}$ and 2800 $cm^{-1}$ which shows five bands at 2970 $cm^{-1}$, 2942 $cm^{-1}$, 2928 $cm^{-1}$, 2893 $cm^{-1}$, and 2868 $cm^{-1}$ with the sign pattern (+, –, –, +, –). The bands below 2950 $cm^{-1}$ were described as bands associated with the C–H vibrations of the methylene groups. The bands above 2950 $cm^{-1}$ were associated with the C–H stretching vibrations due to the vinyl and methyl groups. Later analysis by Singh and Keiderling[15] demonstrated that this interpretation was supported by the Fixed Partial Charge model. In this last work, from the theoretical FPC study, two equatorial rotamers were found. The named EQ(C) (EQ-1 in the current work) was the global minimum on the PES and the most abundant at room temperature. The theoretical VCD spectrum was predicted by taking into account only this EQ(C) rotamer to draw a comparison with the experimental one.

In the previous vibrational analysis, it is shown that a reliable assignment of the experimental IR and Raman spectra of (*R*)-(+)-limonene requires taking into account not only the most stable equatorial rotamer but also all the three equatorials found theoretically. As can be see in Figure 5, our recorded experimental spectra are more complex than those in the previous work by Polavarapu et al.,[14] and more than five bands are observed. Bearing in mind that we are working in the harmonic approximation and the rms obtained in the scaling procedure, it can be seen that, in the same way as the IR and Raman spectra, our theoretical calculations are able to reproduce the experimental VCD spectrum in this region, when the three most stable rotamers are taken into account with their respective rotator strength sign. This fact could be further evidence of the presence of the three rotamers in the liquid phase.

The description of the normal modes in this region from the PED agrees with the previous works.[14,15]

In Figure 5b, the C–H stretchings region using the C–H band pass filter for the region between 3100 $cm^{-1}$ and 2800 $cm^{-1}$ is shown. As can be seen, the most important features observed are those bands that change their intensity with respect to the same region recorded without using it (Fig. 5c). For example, the experimental bands at 3083 and 3013 $cm^{-1}$ become lower in relative intensity. At the same time, the resolution in the region between 2900 and 2875 $cm^{-1}$ increases. Thus, where a positive band and a shoulder appeared at around 2900 $cm^{-1}$ two positive bands at 2889 and 2881 $cm^{-1}$ are present. In addition, the negative band at 3043 $cm^{-1}$ disappears (from our vibrational analysis there cannot be assigned any fundamental to this experimental value) and a new and weak positive band can be found at 3023 $cm^{-1}$ (band not observed in the IR and Raman spectra) assigned to the normal mode 2 of EQ-2 and EQ-3 in our previous vibrational analysis following our scaling calculation.

#### 2.3.2. Spectroscopic region from 2000 $cm^{-1}$ to 800 $cm^{-1}$

The experimental VCD spectrum recorded for the (*R*)-(+)-limonene in the neat liquid phase is displayed in Figure 6 and as can be seen, contains extensive overlap, as in the previous region, in agreement with our vibrational analysis and a previous work by Lipp and Nafie.[16] Our study is focused on the conformers present in the liquid phase of neat (*R*)-(+)-limonene. This fact implies that some regions present a larger IR intensity than suitable (between 0.3 and 0.6 absorbance units) and in the VCD spectrum appears distorted. Thus, our study will be centered in the 1350–900 $cm^{-1}$ region.

As in the previous region, our study is made within the harmonic approximation and our predicted spectrum is obtained by taking into account the three most stable rotamers, the theoretical Boltzmann's population of each one, and the scaled wavenumbers from the scaling procedure with its corresponding rms. Bearing these factors in mind, the predicted spectrum (Fig. 5c) suitably reproduced the experimental one, and is indicative of the presence of the three rotamers in the liquid phase.

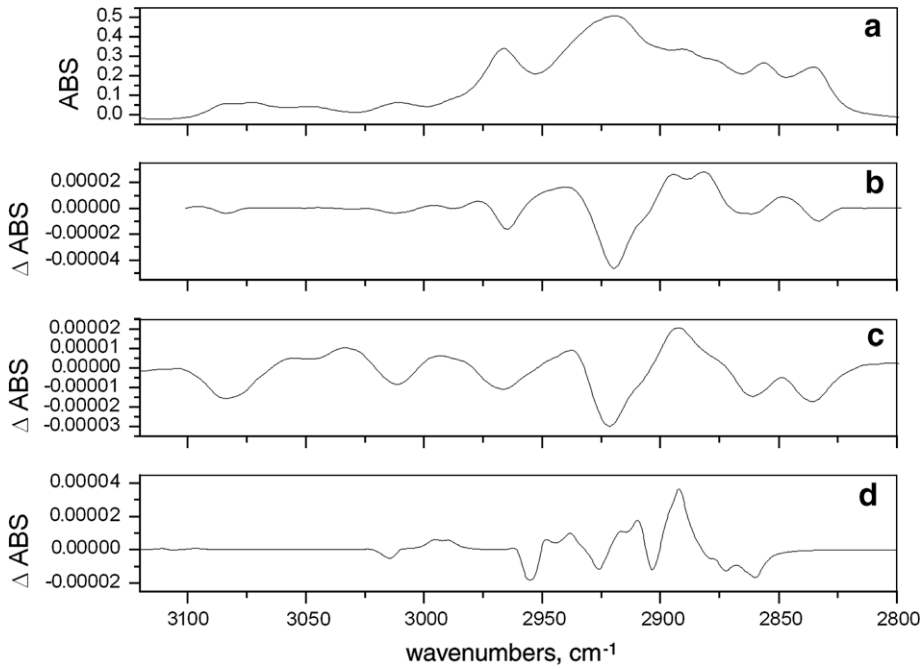


**Figure 5.** Experimental and theoretical spectra of (*R*)-(+)-limonene in the 3200–2800 $cm^{-1}$ region: (a) experimental IR spectrum at 16 $cm^{-1}$ of resolution (neat liquid); (b) experimental VCD spectrum using the C–H band pass filter (8 $cm^{-1}$ of resolution, 7000 scans, neat liquid; (c) experimental VCD spectrum using the standard filter (4 $cm^{-1}$ of resolution, 16,000 scans, neat liquid); (d) theoretical spectrum taking into account contributions of the three most stable rotamers and their theoretical Boltzmann's population at 298 K (obtained using JASCO software,[27] pitch = 1 $cm^{-1}$ and fwhm = 8 $cm^{-1}$).

Our vibrational analysis reveals that the VCD signals in this region are mainly due to methylene motion, although mixed to some extent with the motion of the methyl and vinyl groups and of the ring.

In the above-mentioned work by Lipp and Nafie,[16] the technique of Fourier self-deconvolution was applied to the study of the VCD spectrum of (*R*)-(+)-limonene in order to retrieve concealed information. They expanded three regions, between 1270 and 1210 $cm^{-1}$ (I), between 1180 and 1120 $cm^{-1}$ (II), and between 1060 and 1000 $cm^{-1}$ (III).

The region (I) showed five features upon deconvolution. Following our vibrational analysis in the 1280–1200 $cm^{-1}$ region, these features can be assigned to normal modes 35, 36, and 37 of all the rotamers, and it is this region that can be used to show the presence of different rotamers of *R*-(+)-limonene in the neat liquid phase. (see Tables 2 and 3 for assignment): in the IR and Raman

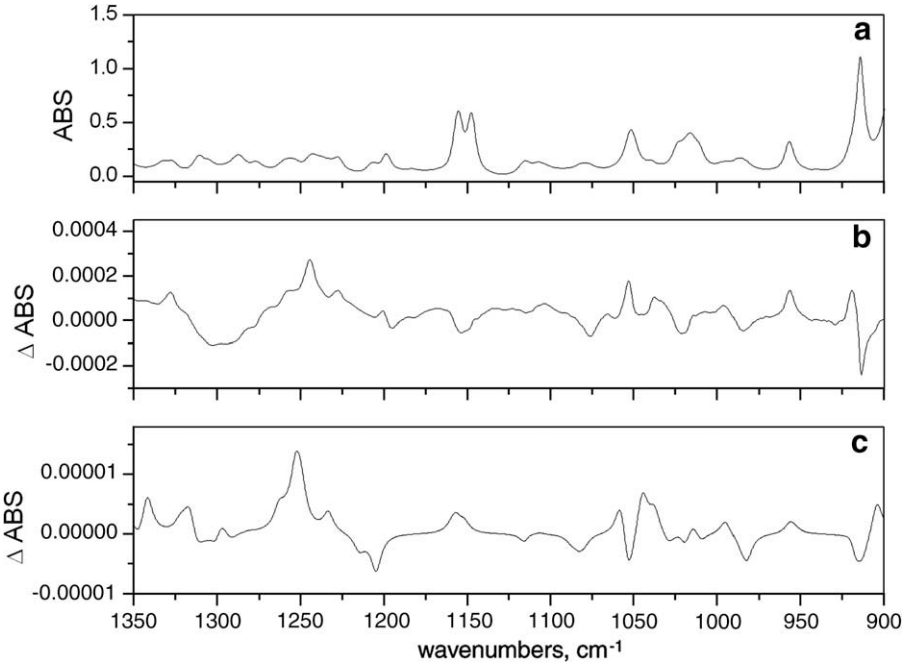


**Figure 6.** Experimental and theoretical spectra of (*R*)-(+)-limonene in the 1350–900 $cm^{-1}$ region: (a) experimental IR spectrum at 16 $cm^{-1}$ of resolution (neat liquid); (b) experimental VCD spectrum (2 $cm^{-1}$ of resolution, 5000 scans, neat liquid); (c) theoretical spectrum taking into account contributions of the three most stable rotamers and their theoretical Boltzmann's population at 298 K (obtained using JASCO software,[27] pitch = 1 $cm^{-1}$ and fwhm = 8 $cm^{-1}$).

spectra, seven bands are present at 1277 $cm^{-1}$ (mode 35 of EQ-1), at 1254 $cm^{-1}$ (modes 35 of EQ-2 and 36 of EQ-1), at 1243 $cm^{-1}$ (mode 36 of EQ-2), at 1227 $cm^{-1}$ (mode 36 of EQ-3), at 1206 $cm^{-1}$ (mode 37 of EQ-1 and EQ-3), and at 1199 $cm^{-1}$ (mode 37 of EQ-2).

In the next region in the study, that is, (II), Lipp and Nafie[16] found a couplet at 1147 $cm^{-1}$ which indicated, according to these authors, the presence of two transitions under this band and a possible coupled oscillator mechanism in effect. Our vibrational study assigns this band only to the normal mode 39 of EQ-3 (described as a methylene scissoring motion). The results of the deconvolution upon the absorbance feature at 1155 $cm^{-1}$ in Ref. 16 indicated a significant amount of remaining overlap in the same way as our vibrational study. In Table 3, it is shown that the normal mode 38 of all the rotamers and 39 of EQ-2 and EQ-3 are assigned to this experimental band. However, our VCD calculation does not reproduce the correct experimental sign. The sign pattern obtained at the B3LYP/cc-pVDZ level is (++−) for modes 35, 36, and 37, respectively, in all the rotamers. In some modes, from the DFT calculation it is found that the positive rotator values are larger than those of the negative ones, and that could be the reason for this disagreement, although a comparative study with similar systems is required to give a more reliable interpretation of it.

Finally, in the last region in the study, in the work by Lipp and Nafie,[16] that is, (III), a couplet at around 1039 $cm^{-1}$ can be found upon deconvolution while the region around 1020 $cm^{-1}$ remained unclear. Our recorded VCD spectrum presents similar absorbance features to that shown in Ref. 16 before deconvolution, but our theoretical study reveals a different pattern. Following our vibrational analysis, in this region, the normal modes 42, 43, 44, 45, and 46 of the three rotamers are assigned (see Table 3). These modes are described as methyl rockings mixed in some cases with C–C stretchings to some extent. The sign pattern obtained for the rotator strength at the B3LYP/cc-pVDZ level is (−+−+−) for EQ-1, (++−++) for EQ-2, and (−+−−+) for EQ-3. The sign pattern and the wavenumbers scaled values jointly give the spectral shape displayed in Figure 6c of the predicted spectrum, where three couplets centered at 1055 $cm^{-1}$, at 1047 $cm^{-1}$, and at 1033 $cm^{-1}$ are predicted. These couplets are due to the contributions of the three rotamers.

## 3. Conclusions

For the first time, three rotamers have been detected in the liquid phase of neat (*R*)-(+)-Limonene using experimental vibrational techniques (IR, Raman, and VCD) and theoretical calculations jointly. Experimental IR and Raman spectra have been reproduced taking into account statistical Boltzmann's population of each of them. The previous vibrational analysis has turned out to be needed if a thorough analysis and interpretation of VCD spectrum features are required. The experimental VCD spectrum has been reproduced taking into account the three rotamers detected using IR and Raman techniques. Couplets in the VCD spectrum of (*R*)-(+)-Limonene are due to the presence of the different rotamers in the liquid phase and not only to coupled motions of the same rotamer. The present work reveals that IR, Raman, and VCD are complementary techniques that can be used to characterize flexible chiral systems which present a complex conformational landscape.

## 4. Experimental details

(*R*)-(+)-Limonene was purchased from Sigma–Aldrich (98% purity) and used without any further purification.

IR spectra in the neat liquid phase of (*R*)-(+)-limonene were recorded at room temperature in a Bruker Vector 22 Spectrophotometer equipped with CsI optics, a Globar source, and a DTGS detector. Standard liquid cells with CsI windows were used, and the spectra were recorded with a resolution of 1 $cm^{-1}$ and 200 scans.

Raman spectra in the neat liquid phase were recorded at room temperature in an FT-Raman Bruker RF100/S spectrometer equipped with a Nd:YAG laser (emission line $\lambda$ = 1064 nm) and a Ge detector cooled to liquid nitrogen temperature. The spectra were recorded with a resolution of 1 $cm^{-1}$ and 200 scans.

The VCD spectra of the (*R*)-(+)-limonene in the neat liquid phase were recorded using a JASCO FVS-4000 FTIR spectrometer equipped with InSb (4000–1900 $cm^{-1}$) and MCTV (2000–800 $cm^{-1}$) detectors. All spectra were recorded using a standard cell equipped with BaF2 windows, with a resolution of 2–16 $cm^{-1}$, with a spacer between 6–50 μm and 3000–16,000 scans, depending on the desirable quality of the spectra obtained. For the 3100–2650 $cm^{-1}$ region, the VCD spectra were also recorded using a C–H band pass filter that was purchased from JASCO Inc.

## 5. Computational details

In the first step, a geometry optimization for both axial and equatorial conformers (depending on the relative position of the isopropenyl group with respect to the ring) was performed at the B3LYP/6-31G(d,p) level of theory as implemented in the GAUSSIAN03 package.[21] Afterwards, a fixed scan of the Potential Energy Surface (PES) of the two molecular structures obtained along the torsions C9–C8–C4–C3 (rotation of the isopropenyl group with respect to the ring, Fig. 1) and H19–C7–C1–C2 (rotation of the methyl group with respect to the ring) was carried out at the same level of theory to obtain the minima on the PES.

The molecular geometry of the equilibrium structures found was then reoptimized at the B3LYP/cc-pVDZ level of theory, the relative energies with the Zero Point Correction (ZPE) were calculated and the molecular populations obtained according to Boltzmann's statistics.

For the analysis of the experimental spectra, the harmonic IR, Raman, and VCD spectra of the most stable conformers were calculated at the same level of theory. In the calculation of the VCD spectrum, Stephens' theory[22,23] was used as implemented in GAUSSIAN03.

In order to achieve the assignment and reproduction of the IR and Raman spectra, Pulaýs SQMFF methodology[24] was implemented starting from the molecular force field calculated at the B3LYP/cc-pVDZ level and using a MOLVIB program[25,26] in such a way that the theoretical wavenumbers obtained for the abovementioned most stable conformers were fitted as far as possible to the experimental ones.

With the results from the previous vibrational analysis, the predicted VCD spectra of the most stable conformers at the same level of theory, and with the aid the MAKEVCD program by JASCO Inc.,[27] the experimental VCD spectrum of pure (*R*)-(+)-limonene was reproduced and interpreted.

## Acknowledgments

Juan Ramón Avilés Moreno thanks the Ministry of Education and Science of Spain for the Post-Doc Grant SB2006-0119. The authors thank the University of Jaén and *Junta de Andalucía* for the financial support. The authors also thank D. Francisco Hermoso Torres for his help in the laboratory.

## References

1. Polavarapu, P. L.; Michalska, D. F.; Back, D. M. *Appl. Spectrosc.* **1984**, *38*, 438–442.
2. Urbanová, M.; Setnička, V.; Volka, K. *Chirality* **2000**, *12*, 199–203.
3. Wagner, K.-H.; Elmadfa, I. *Ann. Nutr. Metab.* **2003**, *47*, 95–106.
4. Crowell, P. L.; Ren, Z.; Lin, S.; Vedejs, E.; Gould, M. N. *Biochem. Pharmacol.* **1994**, *47*, 1405–1415.

5. Ruberto, G.; Baratta, M. T. *Food Chem.* **2000**, *69*, 167–174.
6. McGeady, P.; Wansley, D. L.; Logan, D. A. *J. Nat. Prod.* **2002**, *65*, 953–955.
7. Özer, H.; Sökmen, M.; Güllüce, M.; Adigüzel, A.; Şahin, F.; Sökmen, A.; Kiliç, H.; Bariş, Ö. *J. Agric. Food Chem.* **2007**, *55*, 937–942.
8. Wei, A.; Shibamoto, T. *J. Agric. Food Chem.* **2007**, *55*, 1737–1742.
9. Chastrette, M.; Rallet, E. *Flavour Frag. J.* **1998**, *13*, 5–18.
10. Calogirou, A.; Larsen, B. R.; Kotzias, D. *Atmos. Environ.* **1999**, *33*, 1423–1439.
11. Nunes, F. M. N.; Veloso, M. C. C.; Pereira, P. A. deP.; de Andrade, J. B. *Atmos. Environ.* **2005**, *39*, 7715–7730.
12. Hoffmann, G. G. *J. Mol. Struct.* **2003**, *661–662*, 525–529.
13. Partal Ureña, F.; Avilés Moreno, J. R.; López González, J. J. *J. Phys. Chem. A* **2008**, *112*, 7887–7893.
14. Polavarapu, P. L.; Diem, M.; Nafie, L. A. *J. Am. Chem. Soc.* **1980**, *102*, 5449–5453.
15. Singh, R. D.; Keiderling, T. A. *J. Am. Chem. Soc.* **1981**, *103*, 2387–2394.
16. Lipp, E. D.; Nafie, L. A. *Appl. Spectrosc.* **1984**, *38*, 774–778.
17. Abbate, S.; Longhi, G.; Ricard, L.; Bertucci, C.; Rosini, C.; Salvadori, P.; Moscowitz, A. *J. Am. Chem. Soc.* **1989**, *111*, 836–840.
18. Abbate, S.; Longhi, G.; Givens, J. W., III; Boiadjiev, S. E.; Lightner, D. A.; Moscowitz, A. *Appl. Spectrosc.* **1996**, *50*, 642–643.
19. Abbate, S.; Longhi, G.; Boiadjiev, S.; Lightner, D. A.; Bertucci, C.; Salvadori, P. *Enantiomer* **1998**, *3*, 337.
20. Abbate, S.; Longhi, G.; Santina, C. *Chirality* **2000**, *12*, 180–190.
21. Frisch, M. J.; Trucks, G. W.; Schlegel, H. B.; Scuseria, G. E.; Robb, M. A.; Cheeseman, J. R.; Montgomery, J. A., Jr.; Vreven, T.; Kudin, K. N.; Burant, J. C.; Millam, J. M.; Iyengar, S. S.; Tomasi, J.; Barone, V.; Mennucci, B.; Cossi, M.; Scalmani, G.; Rega, N.; Petersson, G. A.; Nakatsuji, H.; Hada, M.; Ehara, M.; Toyota, K.; Fukuda, R.; Hasegawa, J.; Ishida, M.; Nakajima, T.; Honda, Y.; Kitao, O.; Nakai, H.; Klene, M.;Li, X.; Knox, J. E.; Hratchian, H. P.; Cross, J. B.; Adamo, C.; Jaramillo, J.; Gomperts, R.; Stratmann, R. E.; Yazyev, O.; Austin, A. J.; Cammi, R.; Pomelli, C.; Ochterski, J. W.; Ayala, P. Y.; Morokuma, K.; Voth, G. A.; Salvador, P.; Dannenberg, J. J.; Zakrzewski, V. G.; Dapprich, S.; Daniels, A. D.; Strain, M. C.; Farkas, O.; Malick, D. K.; Rabuck, A. D.; Raghavachari, K.; Foresman, J. B.; Ortiz, J. V.; Cui, Q.; Baboul, A. G.; Clifford, S.; Cioslowski, J.; Stefanov, B. B.; Liu, G.; Liashenko, A.; Piskorz, P.; Komaromi, I.; Martin, R. L.; Fox, D. J.; Keith, T.; Al-Laham, M. A.; Peng, C. Y.; Nanayakkara, A.; Challacombe, M.; Gill, P. M. W.; Johnson, B.; Chen, W.; Wong, M. W.; Gonzalez, C.; Pople, J. A. GAUSSIAN 03, Revision E.01, Gaussian, Inc.: Wallingford CT, 2004.
22. Stephens, P. J.; Devlin, F. J.; Chabalowski, C. F.; Frisch, M. J. *J. Phys. Chem.* **1994**, *98*, 11623–11627.
23. Cheeseman, J. R.; Frisch, M. J.; Devlin, F. J.; Stephens, P. J. *Chem. Phys. Lett.* **1996**, *252*, 211–220.
24. Fogarasi, G.; Pulay, P.. In *Vibrational Spectra and Structure: Ab initio calculation of force fields and vibrational spectra*; Durig, J. E., Ed.; Elsevier, 1985; Vol. 14, pp 125–219. Chapter 3.
25. Sundius, T. *J. Mol. Struct.* **1990**, *218*, 321–326.
26. Sundius, T. *Vib. Spectrosc.* **2002**, *29*, 89–95.
27. Jasco Spectra Manager for Windows™.
28. Egawa, T.; Kachi, Y.; Takeshima, T.; Takeuchi, H.; Konaka, S. *J. Mol. Struct.* **2003**, *658*, 241–251.
29. Mineyama, M.; Egawa, T. *J. Mol. Struct.* **2005**, *734*, 61–65.
30. Neto, N.; Di Lauro, C.; Castellucci, E.; Califano, S. *Spectrochim. Acta* **1967**, *23A*, 1763–1774.
31. Jensen, F. R.; Bushweller, C. H. *J. Am. Chem. Soc.* **1969**, *9*, 5774–5782.
32. Davidovics, G.; Monnier, M.; Aycard, J. P. *C. R. Acad. Sci., Paris C* **1977**, *285*, 233–236.
33. Lauricella, R.; Kéchayan, J.; Bodot, H. *J. Org. Chem.* **1987**, *52*, 1577–1582.
34. Haines, J.; Gilson, D. F. R. *Can. J. Chem.* **1989**, *67*, 941–946.
35. Rivera-Gaines, V. E.; Leibowitz, S. J.; Laane, J. *J. Am. Chem. Soc.* **1991**, *113*, 9735–9742.
36. Lespade, L.; Rodin, S.; Cavagnat, D.; Abbate, S. *J. Phys. Chem.* **1993**, *97*, 6134–6141.
37. Johnson, R. P.; DiRico, K. J. *J. Org. Chem.* **1995**, *60*, 1074–1076.
38. Lapouge, C.; Cavagnat, D.; Gorse, D.; Pesquer, M. *J. Phys. Chem.* **1995**, *99*, 2996–3004.
39. Rodin-Bercion, S.; Lespade, L.; Cavagnat, D.; Cornut, J. C. *J. Mol. Struct.* **2000**, *526*, 343–359.
40. Grimm, K. G.; Kolbe, A. *Spectrochim. Acta* **1968**, *24A*, 1697–1704.